ACCURACY AND FEASIBILITY OF BUBBLE DYNAMIC MEASUREMENTS WITH FOUR-POINT OPTICAL FIBER PROBES

R.V. Fortunati[*1], S. Guet[1], G.Ooms[1], R.V.A. Oliemans[2] and R.F. Mudde[2]

[1]J.M. Burgerscentrum, Delft University of Technology
Laboratory of Aero- and Hydrodynamics
Leeghwaterstraat 21, 2628 CA Delft
The Netherlands

[2]Kramers Laboratory
Delft University of Technology
Prins Bernhardlaan 6, 2628 BW Delft
The Netherlands

ABSTRACT

The measurement of the individual bubble dynamics in a high void fraction bubbly flow is of primary importance for multiphase flow research. In a bubbly flow, gas can be discriminated locally from liquid by applying optical fiber probes. This study investigates the feasibility of the individual bubble velocity determination in a preferential direction, high void fraction bubbly flow by using a geometrical arrangement of four-point optical fiber probes (figure 1). The feasibility of bubble velocity and size determination is studied with a special emphasis on the bubble-selection requirements. Bubbles of 2 to 10 mm are used, while the void fraction ranges up to 25%.

First, the bubble-probe interaction is investigated. Single bubble experiments show that intrusiveness effects are negligible even for low surface tension values, provided that the bubble is approaching the probe centrally, parallel to the probe axis. In high void fraction vertical bubbly pipe flow, the void fraction obtained from the four-point probe central tip is in good agreement with both local single fiber measurements and the area-averaged void fraction obtained from pressure gradient measurements.

A criterion for selecting the bubbles travelling parallel to the axis of the probe is implemented for dense bubbly flow experiments. This criterion is based on the deviation of the individual times of flight from the mean time of flight. The sensitivity of the results on the selection criterion shows that a good compromise can be found between the requirements for the accuracy, the measurement time duration and the number of validated bubbles. In order to confirm the accuracy of such measurements in a vertical high void fraction bubbly pipe flow, the gas volumetric flow rate value is compared with the area-integration of the gas velocity measurements, which shows that meaningful bubble velocity measurements can be achieved by using four-point optical glass fiber probes.

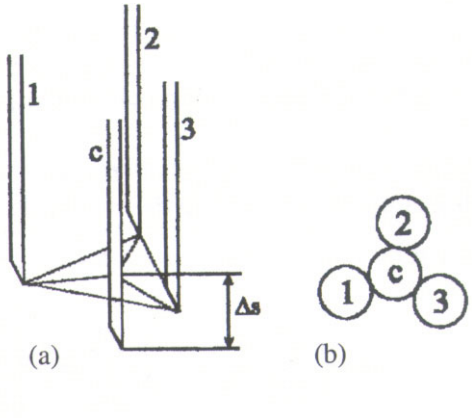

Figure 1: *Four-point optical fiber probe geometry: (a) side view, (b) top view. The respective delay times of the signals on the three peripheral tips (1,2,3) with respect to the central tip (c), the times of flight, are measured and the velocity is calculated using the known distance Δs*

* Corresponding author
Phone: +31 (0) 70 396 26 16

1. INTRODUCTION

The measurement of the bubble dynamics in a dense bubbly flow is of primary importance for multiphase flow research. The present contribution aims at investigating the radial profiles of void fraction and velocities in a high void fraction, vertical bubbly pipe flow.

The measurement of the individual bubble velocity in a high void fraction bubbly flow ($\alpha > 10\%$) is a complicated task. The opacity of the mixture forbids the use of camera-based techniques. Therefore local probes are commonly used. In a bubbly flow, gas can be discriminated locally from liquid by applying optical fiber probes. These optical probes employ the difference in refraction index between gas and liquid. The void fraction can be determined by imposing a threshold value to the optical fiber probe signal. For bubble velocity determination, dual fiber probes are known to provide meaningful results in moderate void fraction flow, based on a time of flight procedure. However, some experimental difficulties remain for high void fraction conditions, i.e. being sure that the two fibers pierce the same bubble (bubbles are known to exhibit spiralling and zig-zagging motions), and relating the local bubble chord length distribution to the individual maximal vertical chord length. Furthermore, the dual fiber probes do not provide information on where a bubble is hit, nor on what the direction of the bubble velocity is. The objective of this project is to measure confidently the bubble velocity radial distribution in a vertical, upward high void fraction bubbly pipe flow. In this contribution the feasibility of such individual bubble velocity measurements is investigated by using a four-point optical glass fiber probe.

First, the principle of four-point probe measurements is explained in section 2, emphasizing on the bubble selection criterion used. Then, in section 3, bubble-probe interactions are investigated by single bubble measurements and comparing the four-point probe measurements with CCD-camera recordings. Next, the sensitivity of the results on the bubble selection criterion is studied in a high void fraction vertical bubbly pipe flow in section 4. Finally, the radial profiles measured in the vertical bubbly pipe flow are presented and compared with gas flow rate measurements to investigate the validity of the measurement procedure.

2. PRINCIPLE OF FOUR-POINT OPTICAL FIBER PROBES

2.1 Gas bubble detection using single optical fiber probes

Placing a glass fiber probe in a bubbly flow allows for the local discrimination between gas and liquid, see Cartellier (1992), Barrau et al. (1999), Leentvaar (2000) and Mudde et al. (2001). The reason for this is the difference in refractive indices. The refractive index going from glass to water is different from the one going from glass to air. Light is sent into the glass fiber and the intensity of reflected light is a measure for the medium in which the optical fiber tip is operating.

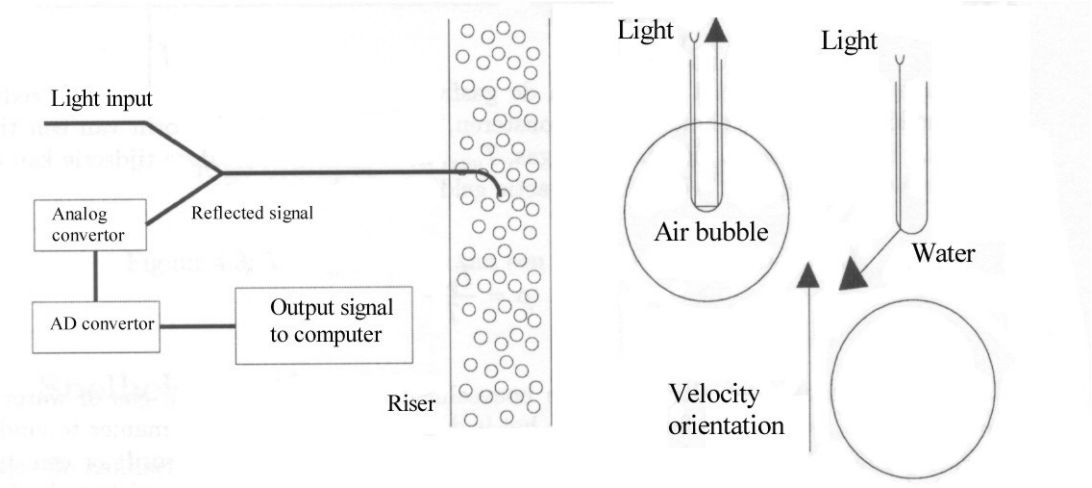

E-mail: rfortunati@planet.nl

Figure 2: *A single point glass fiber probe (left) and the distinction between gas and water by the difference in refractive indices(right). By courtesy of Leentvaar(2000).*

2.2 Four-point probe arrangement

The geometrical arrangement of four-point optical fiber probes permits the calculation of the parallel-to-the-probe velocity component of the gas bubble by using the time of flight of the bubble between a central fiber c, situated upstream (tip c in figure 3) and the 3 other fibers 1,2,3 situated downstream (at Δs = 1.6mm for the four-point-probe used in this contribution). Each fiber has a diameter of 200 μm. The ideal situation is shown at the right-hand side of figure 3. In this case the bubble is assumed to approach the probe vertically and symmetrically with respect to the central tip. This implies that the three individual times of flight τ are equal, or similarly the piercing times associated with fibers 1,2 and 3 are equal (figure 3).

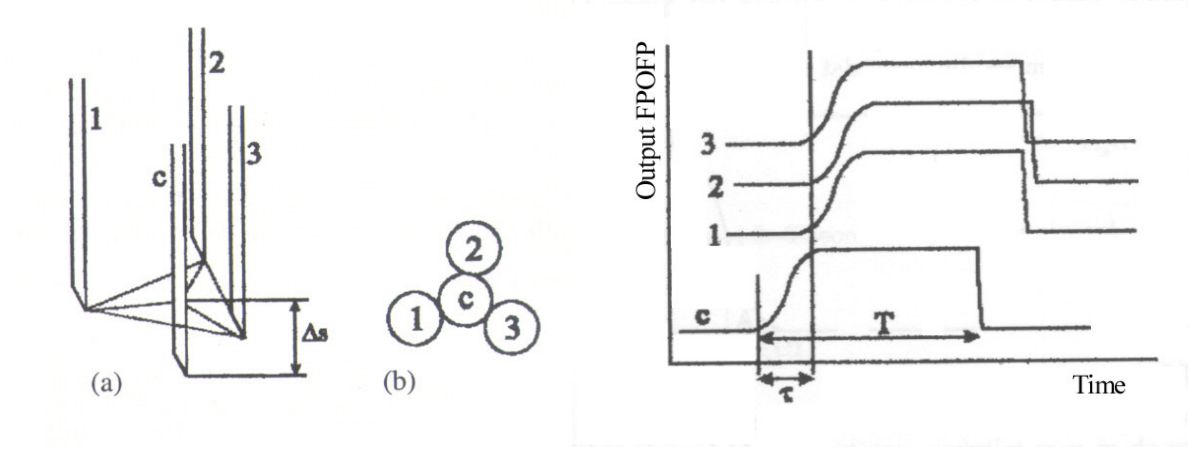

Figure 3: *The four-point optical glass fiber probe (a) side view (b) top view. The probe is oriented downwards in this case. At the right-hand side, the four signals are shown for a vertically upward rising bubble pierced exactly in the axis of the central tip.*

2.3 Time of flight procedure: β-selection criterion

When τ and Δs are known (figure 3), the parallel-to-the-probe velocity is determined by equation {1}:

$$U_g = \frac{\Delta s}{\tau} \qquad \{1\}$$

The bubble vertical chord length follows from the residence time of the central tip in the bubble, T (figure 3):

$$d_B = U_g \cdot T \qquad \{2\}$$

It is more realistic, though, to assume that bubbles do not behave like the ideal situation in vertical upward bubbly pipe flow. First, bubbles not approaching the probe correctly should be filtered from the experimental data. This is done with a criterion on the times of flight τ_1, τ_2, τ_3 for each tip respectively. The mean time of flight τ is defined by equation {3}:

$$\overline{\tau} = \frac{\sum_{i=1}^{3} \tau_i}{3} \qquad \{3\}$$

For a bubble to be selected τ_1, τ_2 and τ_3 should not deviate too much from the mean time of flight $\overline{\tau}$. Physically this means that the bubble is allowed to approach the probe at a bounded angle. Another possibility might be that the centre of gravity of the bubble is shifted with respect to the central tip of the four-point probe up to a certain range. It is most likely that there is a combination of the two. The β-selection criterion defined in equation {4} is used for this purpose:

$$\left| \frac{\tau_i - \overline{\tau}}{\overline{\tau}} \right| < \beta \qquad i = 1,2,3 \qquad 0 < \beta \leq 1 \qquad \{4\}$$

The value of β strongly affects the frequency of selected bubbles. This will be investigated in section 4.4. If the criterion is fulfilled, the three piercing times are used to compute the bubble velocity, see equation {5}:

$$U_g = \Delta s \left(\frac{1}{3} \sum_{i=1}^{3} \tau_i \right)^{-1} \qquad \{5\}$$

Next, the bubble vertical chord length is determined by equation 2. The goal of this feasibility investigation is to study in more details the bubble-probe interaction effects, the influence of the β parameter on the results and the requirements regarding the sampling frequency in order to get reliable, physical results.

2.4 Considerations

2.4.1 Bubble selection criterion

The tolerance on bubble orientation and shift with respect to the probe central tip are bounded by β. For $\beta = 0$, no bubble rotation and/or shift with respect to the probe would be permitted (figure 4a). In that case, it is clear that the vertical diameter of the bubble would be measured. However, in practice the fibers 1,2 and 3 will never pierce the bubble exactly at the same time. Analyzing a continuous signal by using $\beta = 0$ would therefore result in zero selected bubbles. For a certain value of β, the bubbles in figure 4b and 4c would both be selected. Clearly, increasing β results in increasing the spread in the vertical chord length measurements. If the bubble motion is not parallel to the probe (figure 4d), the vertical component of the bubble velocity is determined. A procedure to obtain the optimal value of β will be described in more detail in section 4.4.

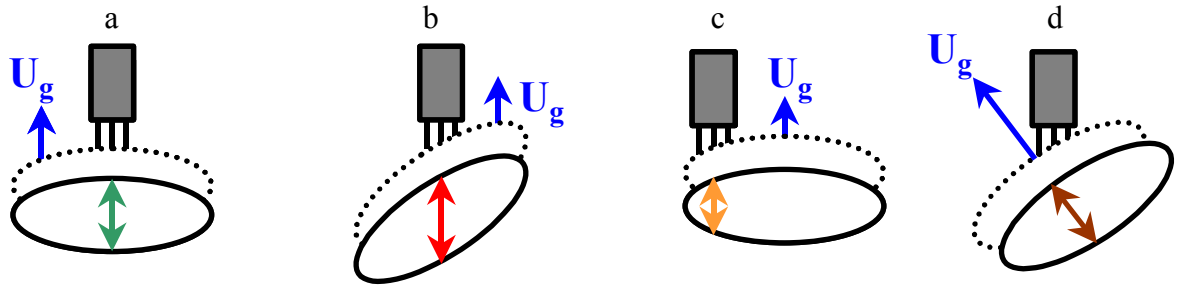

Figure 4: *Bubbles can be either rotated or shifted with respect to the four-point optical fiber probe.*

2.4.2 Local bubble curvature

The bubble velocity and size measurements are, in principle, affected by the bubble curvature. In figure 5, the situation corresponding to a small spherical bubble of radius Δs (figure 5a) is compared with the the flat interface situation of a 'pancake'-shaped bubble (figure 5b). The spherical bubble (figure 5a) travelled a distance of $2\Delta s$ instead of Δs for the pancake bubble. For this reason, depending on the bubble curvature, an additional length δ should be added to Δs in order to give a correct prediction of the bubble rise velocity. Frijlink (1987) proposed equation {6} for the bubble curvature correction (first order approximation):

$$\delta = L - \sqrt{L^2 - l^2} \qquad \{6\}$$

where l is the probe radius and L the first estimate of the bubble curvature.

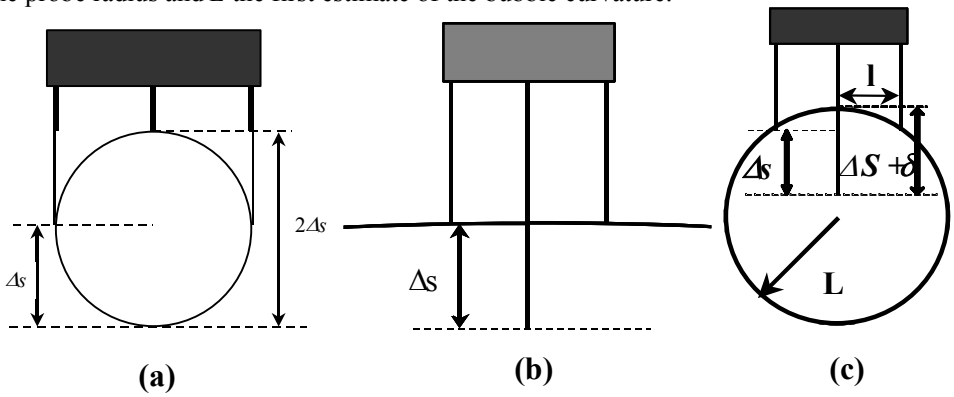

Figure 5: *Schematic representation of the bubble curvature effect (a) for a small spherical bubble; (b) for a flat interface;(c) the correction of vertical distance, Frijlink (1987)*

During the present experiments, the probe radius was r = 0.6 mm and the bubbles were ellipsoidal to pancake shaped with an equivalent spherical diameter of 2 to 10 mm. The bubble curvature effect is therefore neglected, since it leads to a bubble velocity inaccuracy source of less than 2.5 % for the smallest bubbles.

3. SINGLE BUBBLE EXPERIMENTS: INTRUSIVENESS EFFECTS

Before using the probe in a high void fraction bubbly pipe flow, the bubble-probe interaction effects are investigated by measuring the single bubble dynamics using the experimental set-up shown in figure 6. The bubbles are released from a 1 mm diameter nozzle in a 100*160 mm glass box. The bubble trajectories are recorded with a Dalsa 256 CCD camera, providing pictures on a 256 * 256 pixel array at 200 frames per second. The trajectories of single bubbles are tracked at a high frame rate in order to obtain the vertical bubble velocity from a set of successive pictures. The four-point probe is positioned 1 cm above, and in the axis of the nozzle in order to have a stationary bubble motion at the measuring position. Figure 7 represents the comparison between bubble velocity measurements by the four-point probe and bubble velocity measurements by the CCD camera. It is concluded that there is no interaction between the probe and the bubble at the probe location. The inaccuracy of the probe measurements appeared to be even smaller than the pixel resolution of the CCD camera, which was less than 5% in terms of velocity.

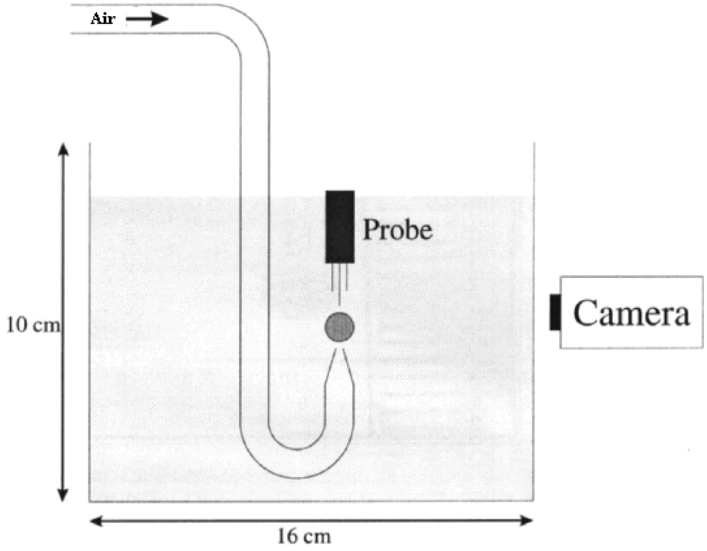

Figure 6: *Single bubbles set-up. The probe detects the bubbles while the probe results for the bubble rise velocity and diameter are checked by the digital CCD camera.*

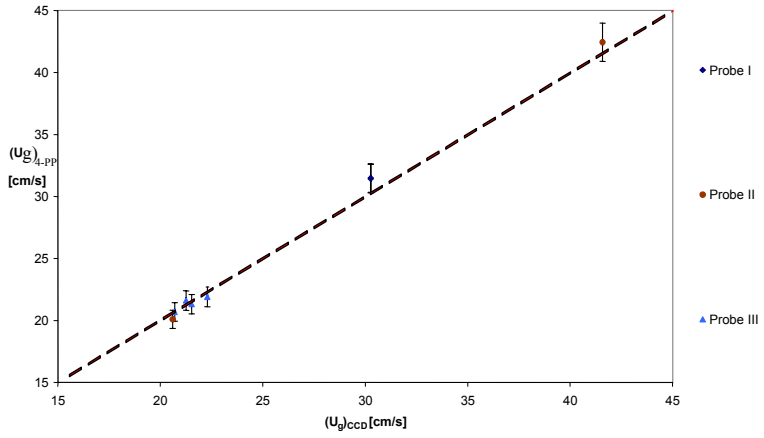

Figure 7: *Four-point probe bubble velocity measurement as a function of the velocity obtained from the CCD camera. The bisector is also plotted.*

The range of bubble sizes implies that the bubbles are ellipsoidal. The equivalent spherical bubble diameter was calculated according to the CCD camera measurements (i.e using the minor and major axis). On the curve proposed by Clift et al. (1978), the bubble velocity measured with the four point probe is plotted versus the estimated equivalent spherical diameter, see figure 8. The results are given by the blue dots for pure water with surface tension $\sigma = 70\ 10^{-3}$ N/m and for water + 0.5% Hexanol by the green dot, with surface tension $\sigma = 35\ 10^{-3}$ N/m. Note that the velocity of the largest bubble is higher than the values from the Clift (1978) curve. This is a consequence of the small distance from the capillary exit to the probe: the wake of the bubble is not fully developed and, hence, the bubble can exceed its terminal velocity.

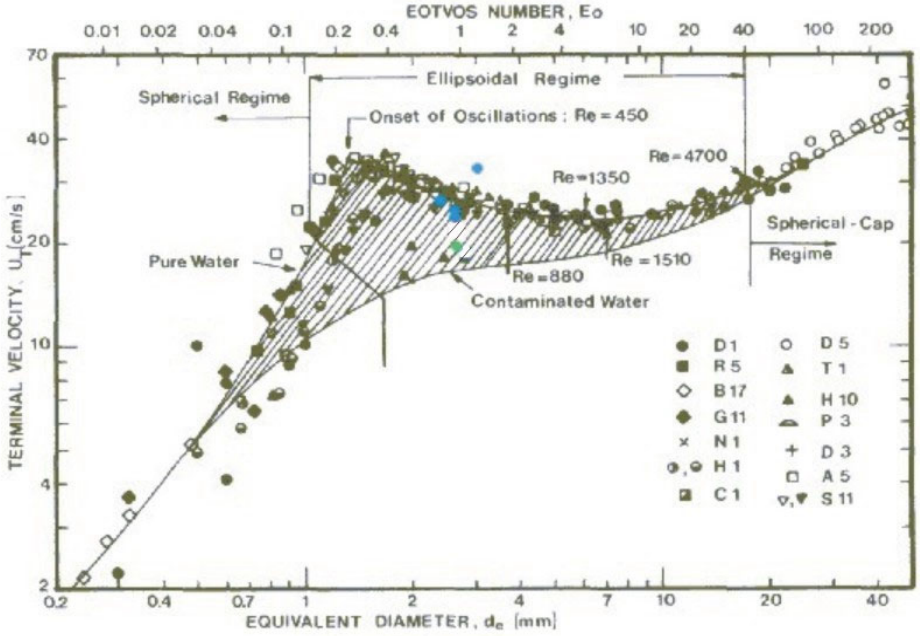

Figure 8: *Terminal velocity of a single bubble vs. its equivalent spherical diameter in an infinite medium according to Clift et al.(1978). The current measurements are also plotted on the curves, for water (blue) and the water-hexanol mixture (green).*

4 HIGH VOID FRACTION BUBBLY PIPE FLOW CONDITIONS

4.1 Experimental set-up

The experimental facility used for the vertical bubbly pipe flow measurements is presented in figure 9. The system consists of a perpex riser (h = 18m ; ID = 72 mm), a returning flow through the downcomer (figure 9, left) and a 200 liters vessel equipped with a centrigal pump to create the liquid recirculation. The gas flow rate is controlled by a Remote Operating Controller, connected to a 100 MHz PC. Six pressure transducers are flush mounted along the pipe wall. Two single optical fibers are inserted at h=4m and 12m, as well as two four point probes at h = 5m and 13m. In that way the void fraction obtained from pressure transducers, single fibers and four-point fibers can be compared. The optical fiber probes signals are sampled at f = 65 kHz using a National instrument GPIB card on a laptop for easy access to the probe location in order to manually adjust the radial traversing mechanisms. A LabVIEW algorithm for the bubble selection procedure has been implemented, as well as for the void fraction determination.

4.2 Surface-averaged void fraction

The void fraction can be measured by means of the following three instrumentational techniques: single optical fiber probes, two pressure transducers up- and downstream and the central tip of four-point optical fiber probes. However, the optical fiber measurements are local measurements and the pressure gradient method gives the volume-averaged void fraction. The cross-sectional averaged void fraction $\langle \alpha \rangle$ can be evaluated from the radial profiles measured by the optical fiber probes according to equation {7}:

$$\langle \alpha \rangle = \frac{1}{\pi R^2} \int_A 2\pi\, r\, \alpha(r) dr \qquad \{7\}$$

where R is the pipe radius, r is the radial position measured from the centreline of the pipe and A is the pipe cross-sectional area.

For the low flow conditions investigated, the friction and acceleration contributions to the pressure gradient are negligible with respect to the hydrostatic pressure gradient. The local mass density of the multiphase mixture follows from equation {8}:

$$\rho = \alpha \rho_g + (1-\alpha)\rho_l \qquad \{8\}$$

Due to the low-pressure conditions, the gas density ρ_g is negligible compared to the liquid density ρ_l :

$$\rho \approx (1-\alpha)\,\rho_l \qquad \{9\}$$

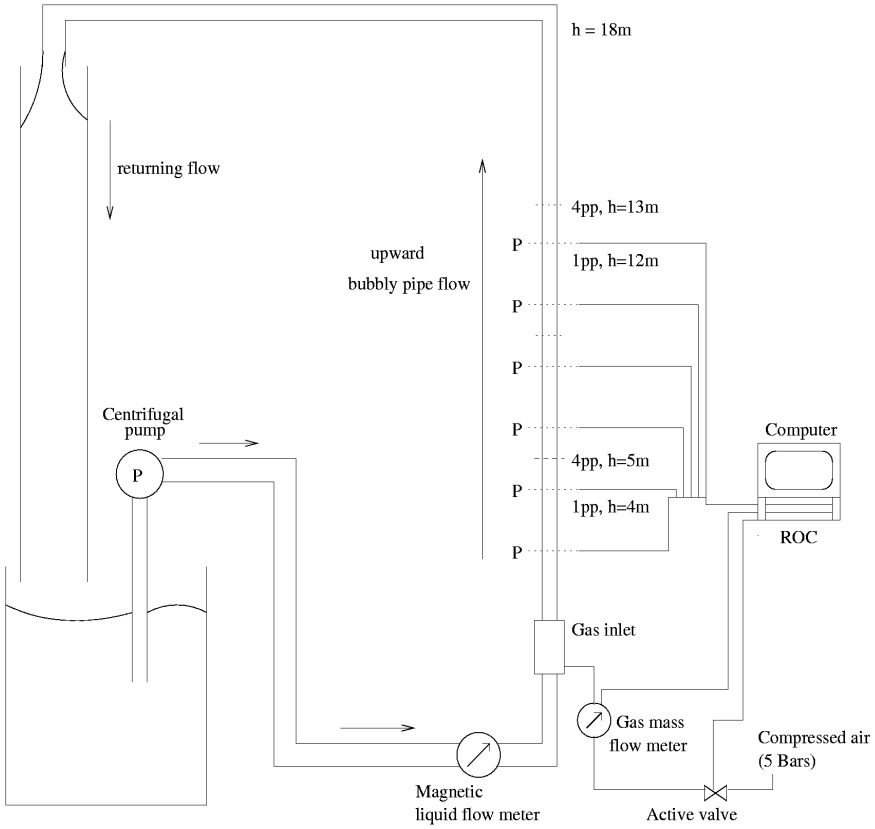

Figure 9: *Gas-lift experimental loop. The riser height is 18 m and the ID is 72 mm. Pressure transducers are present each 2 m up to 12 m. The liquid flow is controlled manually (the flow meter ranges up to 25 l/min), while the gas flow is controlled and metered by means of a link between an active valve and the gas mass flow meter.*

Therefore, the pressure drop can be approximated by equation {10}:

$$\frac{dp}{dz} = (1 - \langle \alpha \rangle)\rho_l\, g \qquad \{10\}$$

Finally, the area-averaged void fraction $\langle \alpha \rangle$ can be estimated by equation {11} using the pressure drop measurements:

$$\langle \alpha \rangle = 1 - \frac{1}{\rho_l g} \frac{dp}{dz} \qquad \{11\}$$

Three types of instrumentation can be compared for area-averaged void fraction measurements: the single- and four-point probe and pressure transducers respectively. Comparison for different flow conditions and pipe axial positions confirm that the four-point probe central tip measures void fraction with confidence, see figure 10.

4.3 Consistency of the measured parallel-to-the probe bubble velocity with gas volumetric flow rate

In order to double-check the accuracy of the four-point probe measurements in general, the volumetric gas flow rate of the gas flow meter was compared with the gas flux detected by the four-point optical fiber probe, according to equation {12}:

$$Q_G = \int_A 2\,\pi\, r\,\alpha(r) U_g(r)\,dr \qquad \{12\}$$

Q_g represents the gas flow rate at the measuring height (i.e. at the local pressure), r is the radial position, α represents the void fraction.

Surface-integration of our local void fraction (α) and bubble rise velocity (U_g) measurements should give the volumetric gas flow rate measured by the gas flow meter. In figure 11 the simultaneous measurements using the gas mass flow meter and the four-point probes are indicated for different flow conditions, showing good agreement.

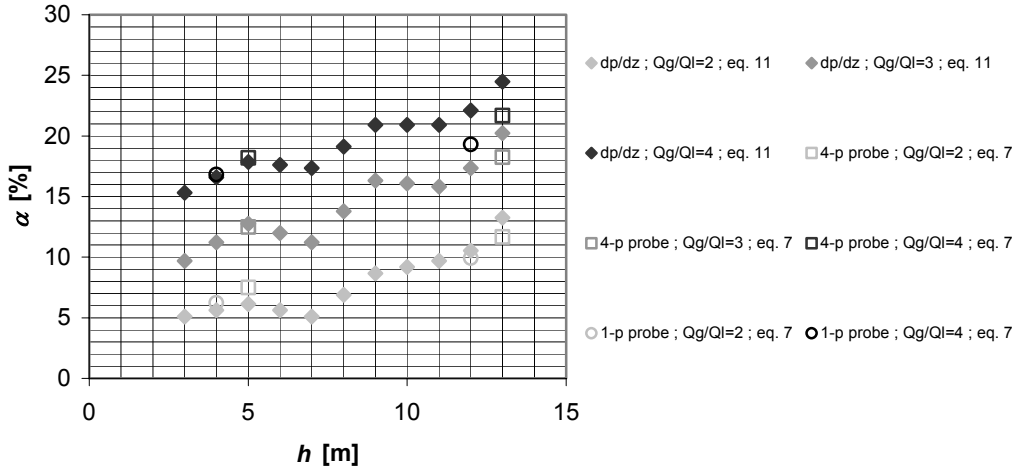

Figure 10: *Comparison of averaged void fraction measurements by means of pressure transducers, single- and four-point optical fiber probes for different flow conditions. The liquid flow rate is constant at 4 l/min.*

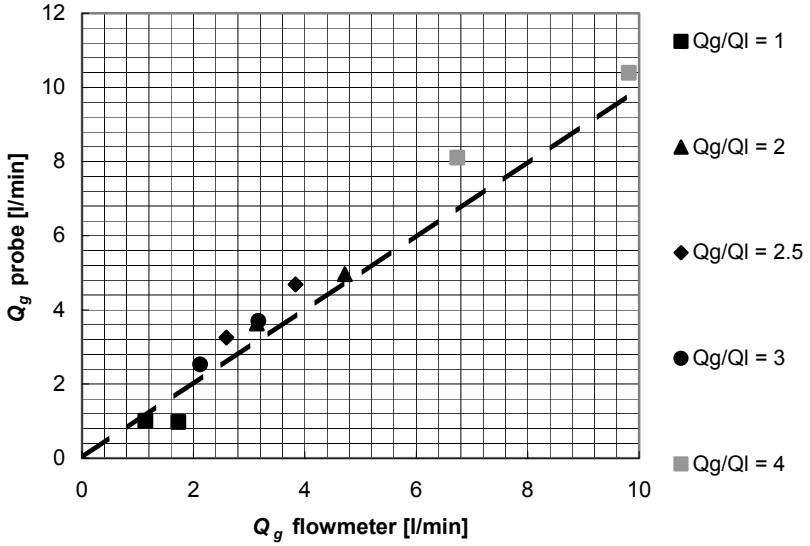

Figure 11: *Consistency of the four-point probe measurements with the gas flow meter measurements. The liquid flow rate was constant (Q_L = 4.00 l/min) while the atmospheric gas flow rate was increased from 4.00 to 16.0 l/min.*

4.4 β Sensitivity Analysis

The influence of the β-parameter on both the relative amount of selected bubbles and the accuracy of the results has been investigated (figures 12 and 13). The analysis has been done for three different flow conditions: the liquid flow rate is fixed to Q_l = 4 l /min, while the gas flow rate is set to three different values. The four-point probe is positioned at the pipe centerline. For three different flow conditions, the sensitivity of the relative number of selected bubbles on the value of the β-parameter is clearly showing the same behaviour, see figure 12. Figure 13 represents probability density functions for the bubble rise velocity at h = 5 m and Q_g/Q_l = 4 for increasing β. It is possible to increase β up to 25 %, without changing the respective probability density functions considerably, cf. figure 13. The other flow conditions exhibit the same behaviour for the β-parameter. It is experimentally found that this limit is corresponding to the maximum slope of the relative amount of selected bubbles, irrespective of the flow conditions chosen. This procedure has been developed for the practicability of the experiments. The measurement time and data file size per local measurement are reduced considerably by introducing this procedure: the feasibility of the experiments is being enhanced.

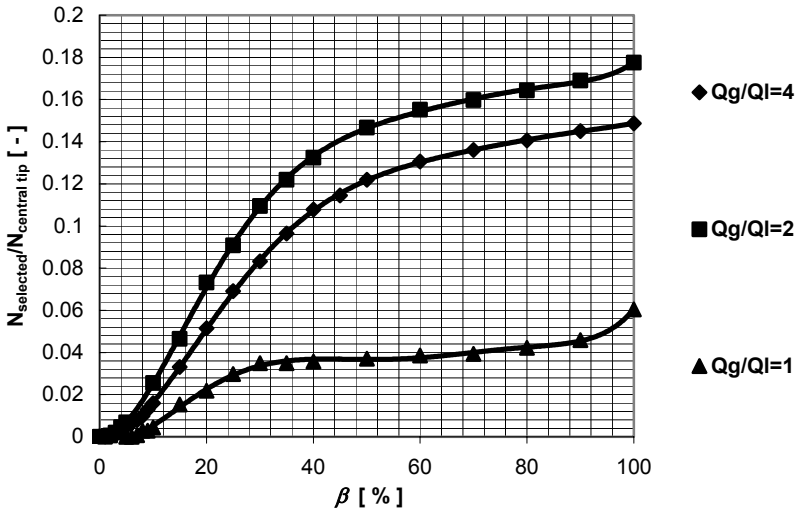

Figure 12: *Relative amount of selected bubbles versus the value of the beta parameter. The relative amount of selected bubbles (y-axis) is the quotient of the number of selected bubbles and the total amount of bubbles pierced by the four-point probe central optical fiber.*

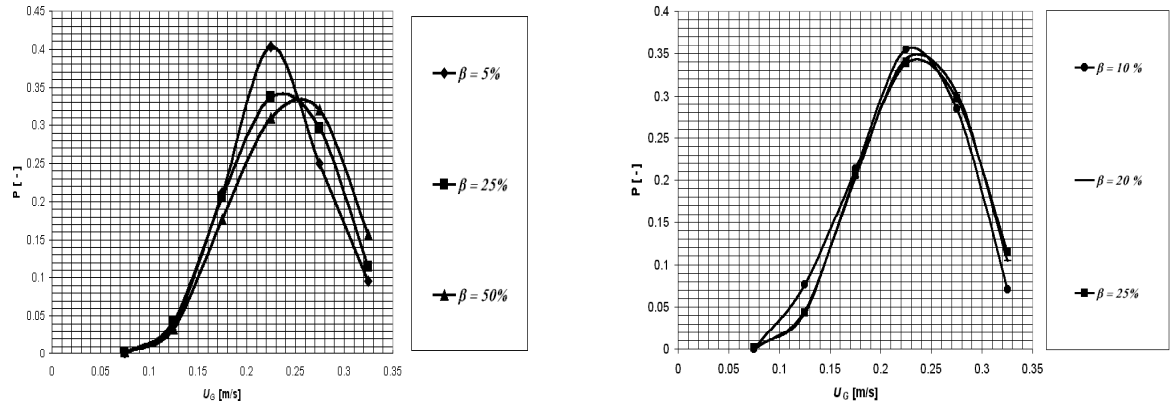

Figure 13: *Probability density functions of vertical bubble velocity for β= 5, 10, 20, 25 and 50 % at Q_g/Q_l=4, h = 5 m. No significant difference is observed on the average rise velocity and its standard deviation for increasing β up to 25 %.*

4.5 Radial distribution of gas velocity in high void fraction bubbly pipe flow

The well-known wall peaking void fraction profile is observed using small bubbles in vertical upward bubbly pipe flow, see figure 14. Liu (1993) and Grossetête(1995) already observed that the associated void fraction

profile is evolving into a core-peaking situation at increased bubble size. At a certain value of the gas flow input, the spatial evolution from a wall peaking to core peaking void fraction profile is observed, see figure 14.

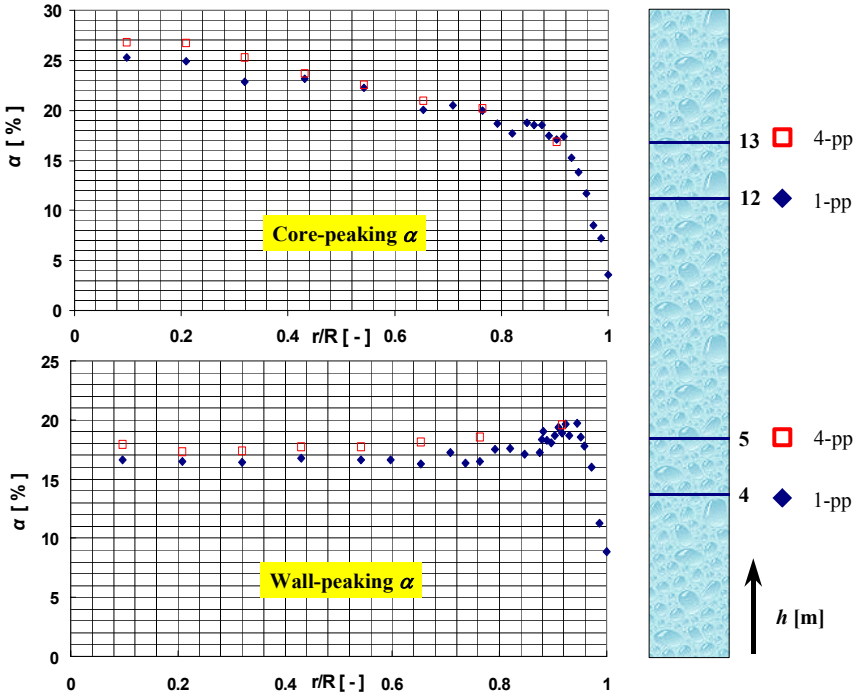

Figure 14: *Spatial evolution of the void fraction profiles at Q_L = 4 l/min and Q_G = 16 l/min. The red symbols show the 4-point probe measurements, while the blue symbols indicate the single fiber measurements.*

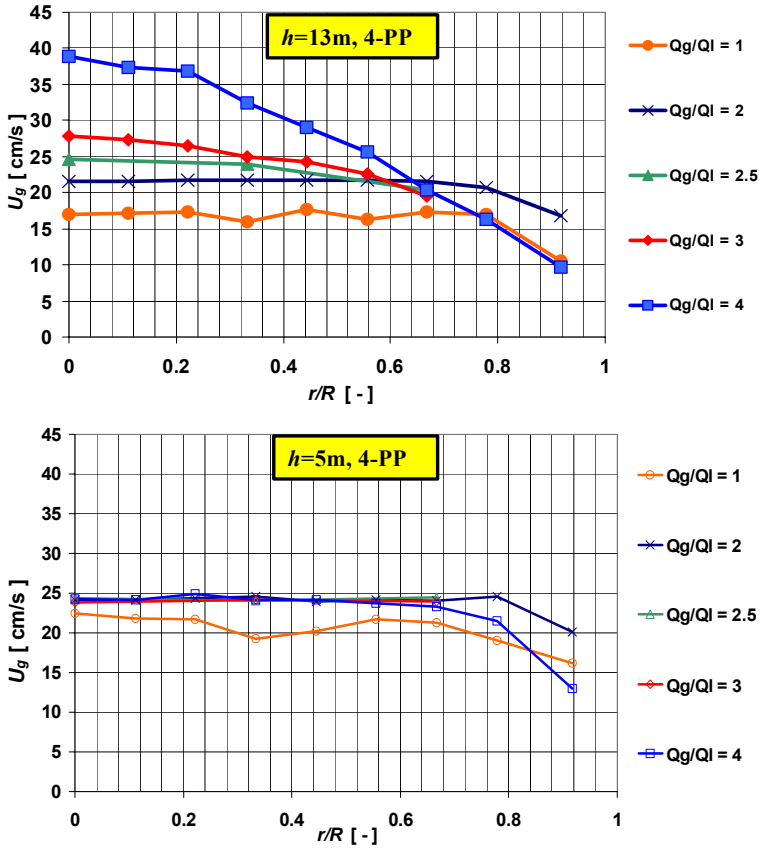

Figure 15: *Spatial evolution of the bubble rise velocity profiles only occurs at Q_g/Q_l = 4.*

The near wall-peaking profile cannot be clearly measured with the four-point probe due to the dimensions of the probe holder (6mm diameter): if the probe housing touches the pipe wall, the central tip registering the void fraction, is still located 3 mm off the wall. The four-point probe is therefore not suitable for the investigation of wall-peaked void fraction profiles. On the other hand, the 4-point probe provides the bubble rise velocity profiles. The spatial evolution from wall-peaking to core-peaking void fraction profile is associated with a transition from a flat to a parabolic profile of bubble velocity, see figure 15.

5. CONCLUSIONS

The purpose of this study was to investigate the feasibility of individual bubble velocity measurements in a high void fraction, preferential direction bubbly pipe flow by using a four-point optical glass fiber probe. From the experimental results, it can be concluded that:

- The bubble – probe interaction effects are absent at the measurements location even though the bubble trajectory might be modified downstream from the probe;
- A good compromise can be found between the number of selected bubbles and the accuracy of the results by using $\beta = 0.25$.
- Bubble rise velocity measurements using four-point optical fiber probes are reliable, according to the consistency with the gas flow meter measurements;
- The four-point probe is a reliable tool for measuring void fraction, considering the comparison with a local measuring method (1pp) and a surface-averaged one (dp/dx method).

The experimental technique developed in this contribution allowed measuring the evolution of the bubble velocity transverse profile. At the wall to core peaking evolution of void fraction profile, the bubble velocity was observed to evolve from a flat to a parabolic profile. In the future the associated evolution of liquid velocity will be investigated using Laser Doppler Anemometry.

Acknowledgements

The experimental facilities were provided by and located at Shell International Exploration and Production in Rijswijk, The Netherlands. The Universiteitsfonds TU Delft granted the funding for participating in this conference.

REFERENCES

1. **Barrau, E., Rivière, N., Poupot, Ch. and Cartellier, A**.; "*Single and double optical probes in air water two-phase flows: real-time signal processing and sensor performance*"; International Journal of Multiphase Flow 25, pp. 229-256, 1999

2. **Cartellier, A.**; "*Simultaneous void fraction measurement, bubble velocity and size estimate using a single optical probe in gas-liquid two-phase flows*"; Rev. Sci. Instrum. 63, pp 5442-5453, 1992

3. **Clift, R. Grace, J.R. and Weber, M.E.**; "*Bubbles, drops and particles*"; Academic press, New York (USA), 1978

4. **Frijlink, J.J.**; "*Physical aspects of gassed suspension reactors*"; Ph.D. Thesis at Delft University of Technology, The Netherlands, 1987

5. **Grossetête, C.**; "*Experimental investigation of void fraction profile development in a vertical cylindrical pipe*"; Advances in Multiphase Flow, 1995

6. **Leentvaar, C.C.W.**; "*Globale en locale hydrodynamica van een air-lift-loop*"; M.Sc. thesis report Kramers Laboratory TU Delft (NL), 2000

7. **Liu, T.J.**; "*Bubble size and entrance length effects on void development in a vertical channel*"; Int. J. Multiphase Flow Vol. 19, No. 1, pp 99-113; Pergamon Press Ltd, Great Britain, 1993

8. **Mudde, R.F., and Saito, T.**; "*Hydrodynamical similarities between bubble column and bubbly pipe flow*"; J. Fluid Mech., 437, pp 203-228, 2001